

Validated Transient Heat-Transfer Model for Underground Transformer in Rectangular Vault

Julien Pierre Albert Sandraz, Francisco de León, *Senior Member, IEEE*, and Joseph Cultrera

Abstract—A new thermal model for underground transformers is proposed in this paper. The model takes the following important characteristics of the transformer installation into account: rectangular shapes; coil and core arrangement; orientation-based convection models for air (vertical, horizontal-upward, and horizontal-downward heat flows); and turbulent or laminar flow regime. The resulting coupled set of differential and algebraic nonlinear equations is solved simultaneously, providing a robust and fast solution that can help design transformers. The model has been validated against three transformers with different dimensions installed in different vaults with onsite measurements. The average absolute difference between the simulated and measured temperatures over several months is typically less than 4 °C. A parameter sensitivity study shows the critical importance of the proper estimation of the full-load heat loss and the ambient soil temperature.

Index Terms—Distribution transformers, heat-transfer transients, predictive maintenance, thermal analysis, thermal circuit.

NOMENCLATURE

Thermal circuit elements on Fig. 1:

C [$\text{J} \cdot \text{K}^{-1}$]	Heat capacity (thermal capacitance).
q [W]	Time-varying heat flow, akin to electric current.
Q [W]	Constant heat flow.
R [$\text{K} \cdot \text{W}^{-1}$]	Thermal resistance.
T [K]	Temperature, akin to electric voltage.

Physical elements of the model (Fig. 1):

A	Air surrounding the system.
CL	Transformer coils.
CR	Transformer core.
Gc	Surrounding ground, closer to the vault (1 ft wide).
Gf	Surrounding ground, farther (20 ft wide).

inf	Ground at “infinity” (out of the reach of the system).
O	Transformer oil.
T	Tank.
V	Vault.

Other variables used in this paper::

A [m^2]	Surface area.
c [$\text{J} \cdot \text{K}^{-1} \cdot \text{kg}^{-1}$]	Isobaric specific heat capacity.
D [m]	Depth (one of the three dimensions).
g [$\text{m} \cdot \text{s}^{-2}$]	Acceleration of gravity on Earth.
h [$\text{W} \cdot \text{K}^{-1} \cdot \text{m}^{-2}$]	Heat-transfer coefficient.
H [m]	Height (one of the three dimensions).
k [$\text{W} \cdot \text{K}^{-1} \cdot \text{m}^{-1}$]	Thermal conductivity.
L [m]	Shape-specific convection scale coefficient.
Nu [\emptyset]	Nusselt number.
P [m]	Perimeter of a given external surface of a solid.
Ra [\emptyset]	Rayleigh number.
s [\emptyset]	Apparent power (transformer loading).
Vol [m^3]	Volume.
W [m]	Width (one of the three dimensions).
α [K^{-1}]	Volumetric thermal expansion coefficient.
ε [\emptyset]	Emissivity coefficient (radiation).
ν [$\text{m}^2 \cdot \text{s}^{-1}$]	Kinematic viscosity.
ρ [$\text{kg} \cdot \text{m}^{-3}$]	Density.
σ [$\text{W} \cdot \text{K}^{-4} \cdot \text{m}^{-2}$]	Stefan–Boltzmann constant.

Other subscripts:

av	Average.
exp	Experimental value.
f	Fluid.
FL	Full load (power losses).
hu	Horizontal-upside convection (fluid above solid).

Manuscript received October 08, 2012; revised February 13, 2013 and April 06, 2013; accepted April 17, 2013. Date of publication May 16, 2013; date of current version June 20, 2013. Paper no. TPWRD-01090-2012.

J. Sandraz and F. de León are with the Department of Electrical and Computer Engineering, Polytechnic Institute of New York University, Brooklyn, NY 11201 USA (e-mail: julien.sandraz@gmail.com; fdeleon@poly.edu).

J. Cultrera is with the Consolidated Edison Company of New York, Inc., New York, NY 10003 USA (e-mail: cultrera@coned.com).

Color versions of one or more of the figures in this paper are available online at <http://ieeexplore.ieee.org>.

Digital Object Identifier 10.1109/TPWRD.2013.2260183

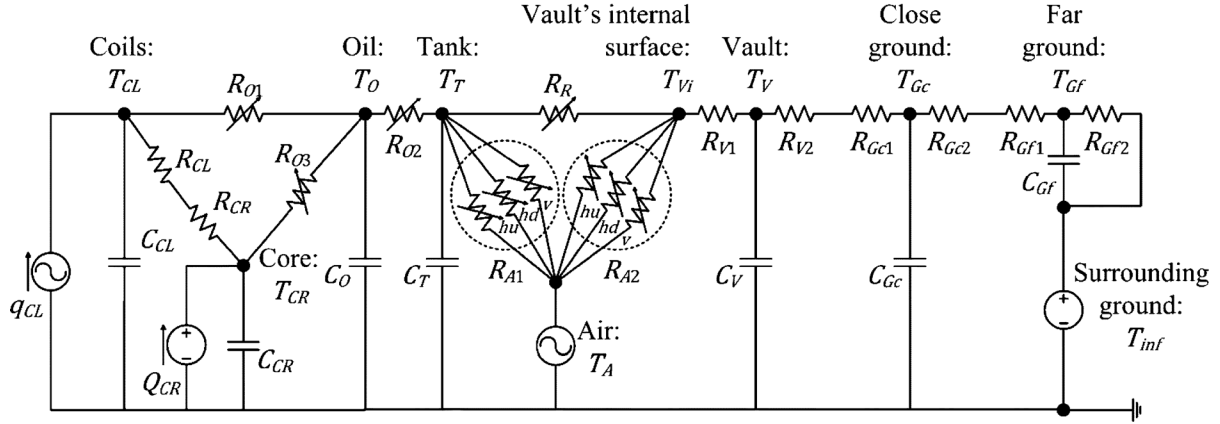


Fig. 1. Thermal circuit representing heat transfers within rectangular underground transformer installations.

- hd* Horizontal-downside convection (fluid below solid).
- i* Inside (internal surface).
- NL No-load (power losses).
- o* Outside (external surface).
- p* Isobaric (at constant pressure).
- p.u. Per unit.
- r* Radiation.
- s* Solid.
- S* Thermal source (power losses).
- v* Vertical (fluid next to vertical solid surface).

I. INTRODUCTION

TRANSFORMERS installed in underground vaults run notably hotter than in the testing facilities at the factory [1]. This is caused by the confinement of the vaults where air convection is reduced. This problem may lead to unexpected reduction in transformer life expectancy [1]. It was found in [2] that 50 kVA units at 150% load installed in standard-size vaults experience an increase in top-oil temperature rise of about 9 °C over those installed in open air.

A thermal model has been proposed in the case of cylindrical distribution transformers in underground vaults in [3]. The study was limited to typical daily load cycles, steady loads, and step loads. Only the effects of earth conductivity and radiation barriers were considered. Parts of the thermal model and method of investigation described in [3] have been used as a reference for the derivation of our model. The differences are clearly highlighted in the following subsections. We make the remark that the results of the model proposed in this paper and those obtained using the model of [3] (without our improvements) present large differences: over 20 °C in the temperature of the core and coils, and over 10 °C in that of the tank.

A. Features of the Proposed Model

The main contribution of this paper is the proposal of a thermal model for transformers installed in vented (open at

the top) underground vaults (see Figs. 1 and 2). The unique characteristics of the models include: 1) orientation-based convection models for air which includes separate equations for vertical, horizontal-upward, and horizontal-downward flows; 2) different flow regime equations (turbulent or laminar) for each of the flows; 3) rectangular geometries (for tanks and vaults) are considered, unlike previous publications; 4) a geometrical model for the coil and core arrangement is included; 5) the coupled differential and algebraic nonlinear equations describing the system make use of a mass matrix that enables their simultaneous computing, using a variable-order multistep solver, based on the numerical differentiation formulas (NDFs) [4].

The equivalent circuit, shown in Fig. 1, is physically consistent since each element represents a construction component of the transformer installation. For example, each resistor represents a path of heat; each capacitor represents the thermal inertia of the mass of the construction component; and the sources represent time-varying gain or loss of heat. All elements representing convection and radiation are nonlinear.

The model proposed in this paper, when merged with precise internal thermal models for transformers (as those available to the manufacturers), can help solve the problem of estimating the hot-spot temperature (and, thus, the loss of life) with better accuracy for transformers installed in underground vaults.

B. Advantages of the Model

The main advantages of the new model with respect to existing models are that it considers the arrangement of the core and coils within the tank (see Figs. 2 and 3) each having a separated temperature variable. The model has been validated in the field against measurements on three transformers in service, each with different installation characteristics. Transformer 1 (rated 500 kVA) has external dimensions of 58 × 30 × 63 in and is installed in a small vault of internal dimensions 84 × 50 × 132 in. Transformer 2 (rated at 1000 kVA) with external dimensions of 81 × 31 × 64 in is installed in a large vault of dimensions 102 × 60 × 162 in. Transformer 3 (rated 500 kVA), with the same external dimensions as transformer 1, is installed in a large vault equal to the one of transformer 2. The transformers

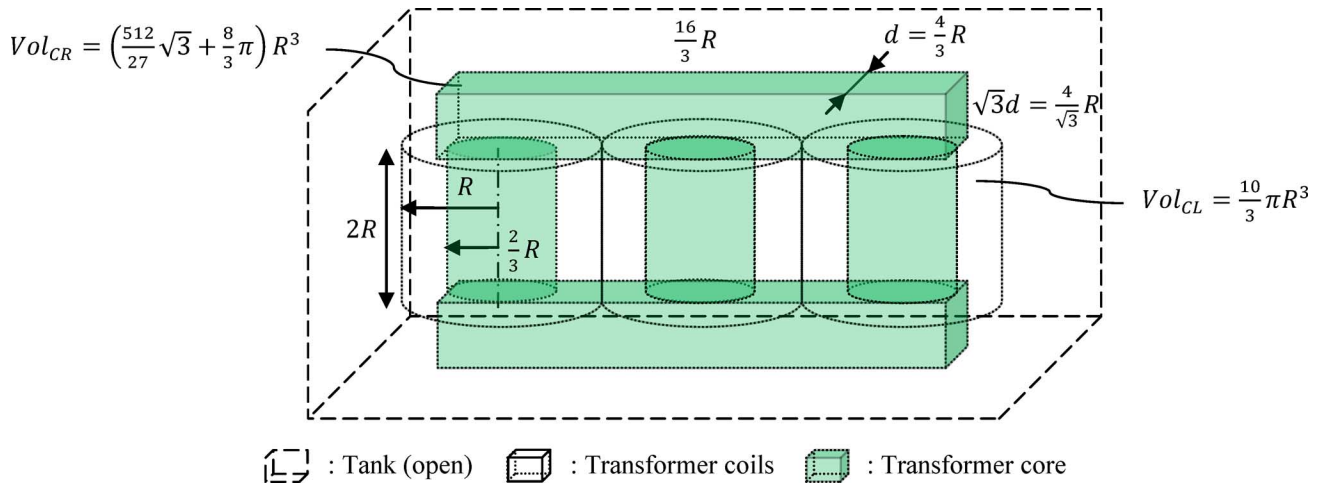


Fig. 2. Geometrical model of the transformer (core and coils).

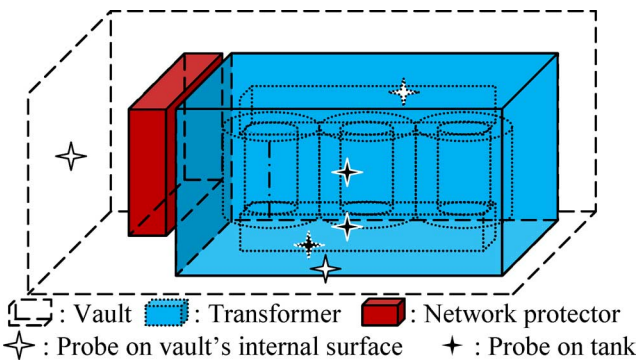


Fig. 3. Transformer 1 in its vault.



Fig. 4. Underground vault below sidewalk, containing Transformer 1.

hang from supports to the wall (effectively suspending the transformer in the air). The separation distance at the bottom and at the back of the transformer is 6 in. The tanks studied, whose surfaces are flat (not corrugated), are centered in the vault along the width of the vault.

The average absolute difference between the simulated and measured temperatures over the entire span of this study (one year) is typically less than 4 °C. A systematic parametric study

was performed to gauge the effect of the uncertainty of the input data. It was found that the most sensitive parameter is the full-load loss followed by the ambient soil temperature.

II. THERMAL MODEL

A. System Definition and Equations

The thermal-electrical analogy enables one to describe heat flow with a lumped-parameter circuit in the same way that an electric current flows. There are three main different mechanisms for heat transfer: conduction between two solids, convection between a solid and its surrounding fluid and radiation between two solids through a fluid. Conduction can be modeled by a constant thermal resistance, but convection and radiation are nonlinear phenomena, which are briefly described below.

The installation under study is represented with a lumped-parameter model taking the average temperature per element. The higher the thermal conductivity, the better this approximation is. Except for the simplified general-purpose geometrical model of the coils and core arrangement (given in Fig. 2), all elements have a rectangular shape. The following differential-algebraic matrix equation represents the system of Fig. 1:

$$M(T) \cdot \frac{dT(t)}{dt} = A(T) \cdot T(t) + B(T) \cdot u(t) \quad (1)$$

with

$$T(t) \triangleq [T_{CL} \ T_{CR} \ T_O \ T_T \ T_{Vi} \ T_V \ T_{Gc} \ T_{Gf}]^T \quad (2)$$

$$u(t) \triangleq [q_{CL}(t) \ Q_{CR} \ T_A(t) \ T_{inf}]^T \quad (3)$$

where

$T(t)$ vector of temperatures (dependent variables), representing each element of the installation;

$u(t)$ vector containing heat fluxes, akin to current sources (inputs) and known temperatures, akin to voltage sources, determined from the system (boundaries);

TABLE I
CONVECTION CONSTANTS' VALUES

Convection		Ra_{L_s}	$K_{f,1}$		$K_{f,2}$		$K_{f,3}$		L_s
			Oil	Air	Oil	Air	Oil	Air	
Vertical		$< 10^9$		0.56		1/4		0.38	H_s
		$\geq 10^9$		0.12		1/3			
Horizontal	Top	$< 10^9$		0.54		1/4		0.5	$\frac{A_{s,hu}}{P_{s,hu}}$ $= \frac{A_{s,hd}}{P_{s,hd}}$ $= \frac{W_s \cdot D_s}{2 \cdot (W_s + D_s)}$
		$\geq 10^9$	0.678	0.14	1/4	1/3			
	Bottom	any		0.25		1/4			

- $M(t)$ mass matrix, a diagonal matrix containing the total thermal capacity of each element over its volume; note that V_i , being a surface, has zero heat capacity; hence, the equation modeling its behavior is, in fact, an algebraic one (see Fig. 10);
- $A(t)$ system's internal dynamics matrix, given in Fig. 11;
- $B(t)$ dynamics of the interaction between the input or boundaries of the system in $u(t)$ and the system variables in $T(t)$ (see Fig. 10).

B. Convective Heat Transfer Model [5]

All nonlinear thermal resistances in Fig. 1 symbolize a convective heat transfer, except R_r , which models the radiated heat from tank to wall. They all vary with temperature. The conduction between solid s and fluid f across surface A_f is governed by the following equations:

$$\frac{1}{R_f} \triangleq h_f \cdot A_s \quad (4)$$

$$Nu_{L_s} \triangleq \frac{h_f \cdot L_s}{k_f(T_{av})} = K_{f1} \cdot [Ra_{L_s}(T_{av})]^{K_{f2}} \quad (5)$$

$$Ra_{L_s} \triangleq \frac{g \cdot \rho_f(T_{av}) \cdot \alpha_f(T_{av}) \cdot c_{p,f}(T_{av}) \cdot |\Delta T| \cdot L_s^3}{k_f(T_{av}) \cdot \nu_f(T_{av})} \quad (6)$$

$$T_{av} \triangleq K_{f3} \cdot T_f + (1 - K_{f3}) \cdot T_s \quad (7)$$

where

T_{av} average temperature representative of the temperature of the fluid (f) in close proximity to solid (s);

$|\Delta T| = |T_s - T_f|$ absolute temperature difference;

K_{f1} , K_{f2} , and K_{f3} empirically determined constants (see Table I).

The values of the material's properties, functions of T_{av} , have been taken from the library of the finite-elements software Comsol 3.5 [6]. The values of the convection parameters described before are given in Table I. The condition on Ra_{L_s} defines the nature of the flow: for $Ra_{L_s} < 10^9$, the flow is said to be laminar, and for $Ra_{L_s} \geq 10^9$, the flow is said to be

turbulent. Note that the expressions given for L_s are not valid for the transformer core and coils because their geometry is not rectangular; the correct values can be found in Table IV.

C. Radiative Heat-Transfer Model

In the case of the radiation between the surface of the tank T facing the internal surface of the vault V_i , through the air, we have [5]

$$\frac{1}{R_r} \triangleq h_r \cdot A_{To:Vi} \quad (8)$$

$$h_r \triangleq \frac{\sigma \cdot (T_T^2 + T_{Vi}^2) \cdot (T_T + T_{Vi})}{\frac{1}{\varepsilon_T} + \frac{1}{\varepsilon_V} - 1} \quad (9)$$

where

$A_{To:Vi}$ area of the tank facing the vault;

h_r radiative heat coefficient between two parallel plane surfaces.

III. EXPERIMENTAL SETUP

A. Measured Temperatures

In order to validate the proposed thermal model, three underground transformers, connected to the New York City distribution grid have been selected. Temperature probes have been installed on both the vault's internal surface and the transformer tank's external surface (positions marked on Fig. 3).

The raw output of the probes has been used to calculate a weighted average temperature of the tank $T_{T,exp}(t)$ and of the vault's internal surface $T_{Vi,exp}(t)$. The weight is given by the relative area of which each probe is representative to the total area of the element (tank or vault). This data is shown in the following section when compared to simulated temperatures.

B. Simulation Input and Boundary Data

The system is driven by the inputs specified by $u(t)$ in (3): the transformer resistive heat loss. It is established that the loss distribution is the following:

$$q_{CL}(t) = (Q_{FL} - Q_{NL}) \cdot s_{av,p.u.}(t) \quad (10)$$

$$Q_{CR} = Q_{NL} \quad (11)$$

where

Q_{FL} full-load transformer loss;

Q_{NL} no-load loss;

$s_{av,p.u.}(t)$ recorded several times per hour at random times.

Also, an average city-wide hourly air temperature, recorded by meteorological services, has been used as the ambient air temperature T_A . The data for both is shown together with the results.

IV. RESULTS AND MODEL VALIDATION

Only a selection of the graphs and analyses regarding mostly Transformer 1 are presented in this paper. The data from the

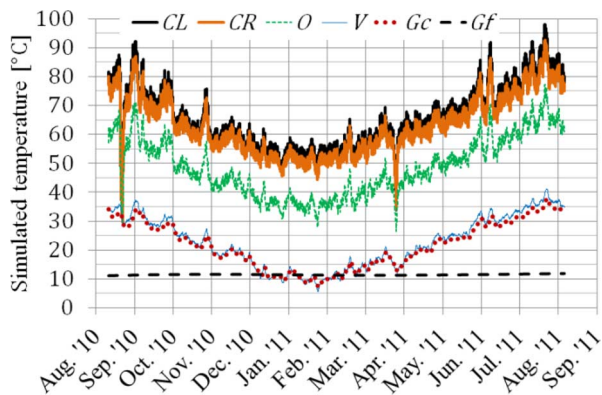


Fig. 5. Simulation outputs: $T(t)$ as described in (2), without T_T or T_{Vi} .

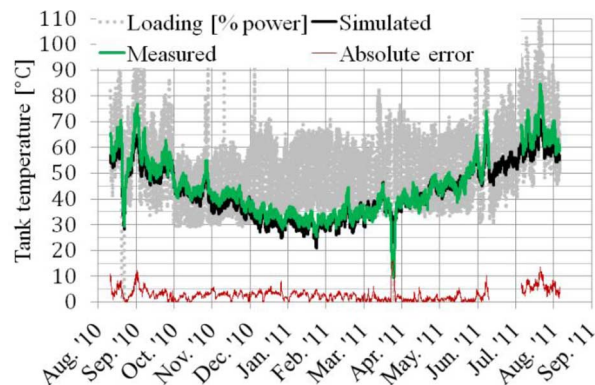


Fig. 6. Tank: measured/simulated temperature comparison.

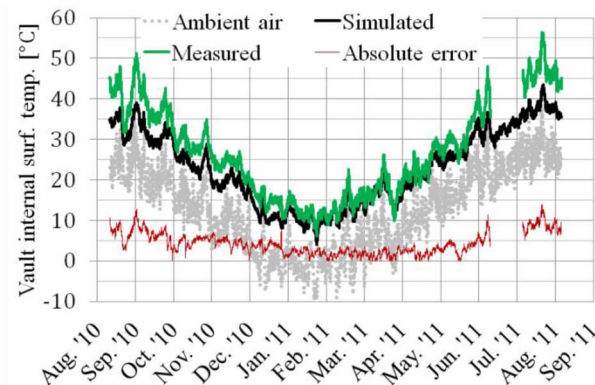


Fig. 7. Vault's internal surface: measured/simulated temperature comparison.

other two transformers confirms the conclusions drawn from the first one.

A. Simulation Data

The simulated temperatures of each system element (all but tank and vault) for a 12-month period is given in Fig. 5. Note that there are two temperature dips (August 2011 and March 2012) corresponding to times where the network protectors opened. Fig. 6 compares the simulated and measured temperature of the tank; the trend follows the transformer loading. Fig. 7 compares the measured versus simulated temperature of the vault. The

TABLE II
SIMULATION RESULTS COMPARED TO MEASUREMENTS

Transformer		#1	#2	#3	
Rated power [kVA]		500	1000	500	
Vault size		smaller	larger	larger	
Period		Summer 2010 to summer 2011	Summer 2011	Summer 2011	
Error on average temperatures [°C]	absolute	Tank	Average: 2.6 Winter: 2.3 Spring: 1.9 Summer: 5.2 Fall: 2.7	9.1	1.3
		Vault interior	Average: 3.9 Winter: 2.0 Spring: 3.0 Summer: 8.1 Fall: 4.6	1.3	3.9
	relative	Tank	-2.1	+9.1	+0.5
		Vault interior	-3.9	-0.5	-3.8

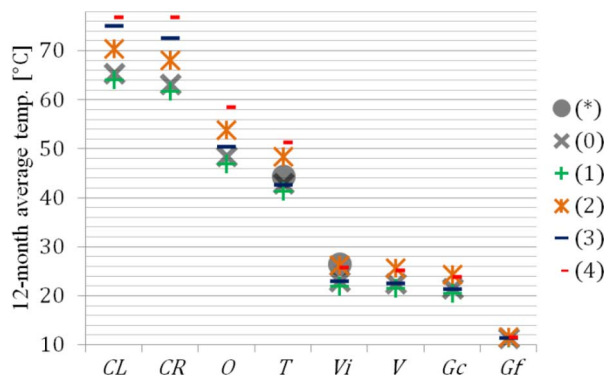


Fig. 8. Average simulated temperatures without single features compared to fully featured (reference) simulation.

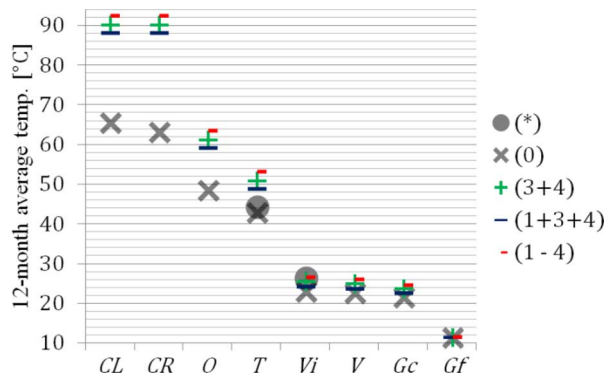


Fig. 9. Average simulated temperatures without groups of features compared to fully featured simulation.

trend follows the ambient temperature $T_A(t)$. All temperatures follow both T_A and the transformer loading.

B. Comparison With Measurements

The simulated and measured tank temperatures, as well as the absolute difference between the two, can be seen in Fig. 6, for each half-hour of the 12-month study period. The differences are

$$M(T) \cdot \frac{dT(t)}{dt} = A(T) \cdot T(t) + B(T) \cdot u(t) \Leftrightarrow \begin{bmatrix} C_{CL} & 0 & 0 & 0 & 0 & 0 & 0 & 0 \\ 0 & C_{CR} & 0 & 0 & 0 & 0 & 0 & 0 \\ 0 & 0 & C_o(T_o) & 0 & 0 & 0 & 0 & 0 \\ 0 & 0 & 0 & C_T & 0 & 0 & 0 & 0 \\ 0 & 0 & 0 & 0 & \boxed{0} & 0 & 0 & 0 \\ 0 & 0 & 0 & 0 & 0 & C_V & 0 & 0 \\ 0 & 0 & 0 & 0 & 0 & 0 & C_{Gc} & 0 \\ 0 & 0 & 0 & 0 & 0 & 0 & 0 & C_{Gf} \end{bmatrix} \cdot \frac{d}{dt} \begin{bmatrix} T_{CL}(t) \\ T_{CR}(t) \\ T_o(t) \\ T_T(t) \\ T_{Vi}(t) \\ T_V(t) \\ T_{Gc}(t) \\ T_{Gf}(t) \end{bmatrix} = A(T) \cdot \begin{bmatrix} T_{CL}(t) \\ T_{CR}(t) \\ T_o(t) \\ T_T(t) \\ T_{Vi}(t) \\ T_V(t) \\ T_{Gc}(t) \\ T_{Gf}(t) \end{bmatrix} + \begin{bmatrix} 1 & 0 & 0 & 0 & 0 & 0 & 0 & 0 \\ 0 & 1 & 0 & 0 & 0 & 0 & 0 & 0 \\ 0 & 0 & 0 & 0 & 0 & 0 & 0 & 0 \\ 0 & 0 & h_{A1,hu} \cdot A_{To,hu} + h_{A1,hd} \cdot A_{To,hd} + h_{A1,v} \cdot A_{To,v} & 0 & 0 & 0 & 0 & 0 \\ 0 & 0 & h_{A2,hu} \cdot A_{Vi,hu} + h_{A2,hd} \cdot A_{Vi,hd} + h_{A2,v} \cdot A_{Vi,v} & 0 & 0 & 0 & 0 & 0 \\ 0 & 0 & 0 & 0 & 0 & 0 & 0 & 0 \\ 0 & 0 & 0 & 0 & 0 & 0 & 0 & 0 \\ 0 & 0 & 0 & 0 & 0 & 0 & 0 & 1/R_{Gf2} \end{bmatrix} \cdot \begin{bmatrix} (Q_{FL} - Q_{NL}) \cdot s_{av,pu}(t) \\ Q_{NL} \\ T_A(t) \\ T_\infty \end{bmatrix}$$

Fig. 10. Differential-algebraic matrix equation.

consistently below 10 °C during July and August, and below 5 °C throughout the rest of the year, except for very narrow peaks (rain, strong wind, feeder disconnection, etc.).

In the case of the vault, the same curves are given (Fig. 7). The error is consistently below 7 °C from October to May and below 10 °C from June to September, except for some short periods.

Absolute and relative errors on average temperatures, as well as absolute error on peak temperatures, for both tank and vault, for all three transformers, are given in Table II.

In the case of transformer 1, both yearly and seasonally absolute errors on average temperature are shown. Except for the case of tank of transformer 2 (large transformer in large vault), the absolute error on average temperatures for the whole period are between 1.3 and 3.9 °C.

Note that a more detailed model of the internals of the tank as described in [7] has been implemented as well, resulting in a slight improvement (about 0.1 °C) of the data of Table II.

C. Radiation Versus Convection

From the simulation results, it can be observed that radiation accounts for about 60% of the heat transferred from the tank to its surroundings (air or vault). Approximately 40% of the total heat transfer is through natural convection. As mentioned before the transformer hangs from supports on the wall, therefore there is no heat transfer by conduction at the bottom.

V. PERTINENCE OF MODEL COMPONENTS

A. Contribution of Single Model Components

In this section, the relative importance of the different components of the model are obtained by comparing the average simulated temperatures of the complete model (Fig. 1) with those obtained by disabling one component at a time. The outcome of this study is presented in Fig. 8, whose description is given:

- (*) measurements: weighted average of probe data;
- (0) full model: reference average simulated temperatures;

- (1) removal of orientation-dependent air convection model, replaced with the values most used: those for convection between the vertical surface of a solid and the surrounding fluid; all elements are affected (except *Gf*) by only about 2 °C;
- (2) removal of laminar-turbulent air flow regime distinction based on Rayleigh's number, replaced with the values most used: those characterizing the laminar flow; the elements most affected are *CL*, *CR*, *O*, *T*;
- (3) removal of temperature-dependent material model parameters: replaced with their values at room temperature (20 °C). The elements most affected are *CL* and *CR*;
- (4) removal of the transformer core and coils arrangement model: replaced with a simple heat source inside of a cube whose material properties reflect both that of the core and coils; the elements most affected are *CL*, *CR*, *O*, *T*; note that in this case, the same temperature is shown for *CR* and *CL* in Figs. 8 and 9: these two elements are replaced with only one.

One can notice that the effect of simplification (1) is to lower the average temperature of the system elements. This is so because having vertical convection improves the heat dissipation since the colder fluid is not in the way of the hotter fluid being lifted upwards by buoyancy and, thus, it can easily move up (horizontal-upwards case). The same can be said about the horizontal-downward case.

The effect of simplifications (2) and (3) is opposite: having a laminar regime only limits the heat flow (the turbulent regime is capable of transferring more heat to the fluid); using material properties at room temperature (lower than T_{av} the majority of the time) is equivalent to using a material with reduced dissipation properties.

$$\begin{array}{cccccccc}
\boxed{\begin{array}{c} 1 \\ -\frac{1}{R_{CL}+R_{CR}} \\ -h_{O1}A_{CL} \end{array}} & \frac{1}{R_{CL}+R_{CR}} & h_{O1}A_{CL} & 0 & 0 & 0 & 0 & 0 \\
\frac{1}{R_{CL}+R_{CR}} & \boxed{\begin{array}{c} 1 \\ -\frac{1}{R_{CL}+R_{CR}} \\ -h_{O3}A_{CR} \end{array}} & h_{O3}A_{CR} & 0 & 0 & 0 & 0 & 0 \\
h_{O1}A_{CL} & h_{O3}A_{CR} & \boxed{\begin{array}{c} -h_{O1}A_{CL} \\ -h_{O3}A_{CR} \\ -h_{O2}A_{Ti} \end{array}} & h_{O2}A_{Ti} & 0 & 0 & 0 & 0 \\
0 & 0 & h_{O2}A_{Ti} & \boxed{\begin{array}{c} -h_{O2}A_{Ti} \\ -h_{A1,hu} \cdot A_{To,hu} \\ -h_{A1,hd} \cdot A_{To,hd} \\ -h_{A1,v} \cdot A_{To,v} \\ -h_R A_{To} \end{array}} & h_R A_{To} & 0 & 0 & 0 \\
0 & 0 & 0 & h_R A_{To} & \boxed{\begin{array}{c} -h_R A_{To} \\ -h_{A2,hu} \cdot A_{Vi,hu} \\ -h_{A2,hd} \cdot A_{Vi,hd} \\ -h_{A2,v} \cdot A_{Vi,v} \\ -\frac{1}{R_{V1}} \end{array}} & \frac{1}{R_{V1}} & 0 & 0 \\
0 & 0 & 0 & 0 & \frac{1}{R_{V1}} & \boxed{\begin{array}{c} -\frac{1}{R_{V1}} \\ -\frac{1}{R_{V2}+R_{Gc1}} \end{array}} & \frac{1}{R_{V2}+R_{Gc1}} & 0 \\
0 & 0 & 0 & 0 & 0 & \frac{1}{R_{V2}+R_{Gc1}} & \boxed{\begin{array}{c} \frac{1}{R_{V2}+R_{Gc1}} \\ -\frac{1}{R_{Gc2}+R_{Gf1}} \end{array}} & \frac{1}{R_{Gc2}+R_{Gf1}} \\
0 & 0 & 0 & 0 & 0 & 0 & \frac{1}{R_{Gc2}+R_{Gf1}} & \boxed{\begin{array}{c} \frac{1}{R_{Gc2}+R_{Gf1}} \\ -\frac{1}{R_{Gf2}} \end{array}}
\end{array}$$

Fig. 11. Matrix $A(t)$.

B. Cumulative Contribution of Groups of Components

The cumulative effect of removing several features of the model is presented in Fig. 9. We successively removed:

- (3+4) both the temperature-dependent material model and transformer core and coils model;
- (1+3+4) the features removed before, plus the orientation-dependent air convection model;
- (1-4) the features removed before, plus the laminar-turbulent air-flow regime distinction; note that this configuration is the one that would resemble the most that of the model of [3], except that the oil kinematic viscosity ν_O in it is temperature dependent and that, being a vertical axisymmetrical model for cylindrical installations, not only has an outer ground layer but both (Gc and Gf) are in contact with the boundary condition T_{inf} .

The elements most affected for all three cases are CL , CR , O , T . The cumulative effect is very significant, underlying the

necessity to take into account all of the phenomena modeled by the system, and the impracticality to achieve good accuracy with a steady-state linear model.

VI. PARAMETRIC ANALYSIS

Looking at the thermal model of Fig. 1, one can realize that large amounts of physical data are needed to compute the parameters of the circuit. Frequently, however, the information is not available or large uncertainties in their values occur. A parametric study has been carried out in this section to find the sensitivity of each parameter. The idea is to locate which parameters affect the results the most so that efforts can be focused on obtaining these values with the highest precision possible.

We have studied the sensitivity of the full-load loss, oil level, thermal conductivity of the ground, average temperature of the ground (boundary condition), no-load heat loss, ground farther layer's thickness (Gf), and tank thickness. In order to establish the parameters for which a precise determination is critical, the variation of the peak temperatures of each elements corresponding to a given variation of each parameter is tabulated in Table III.

TABLE III
SENSITIVITY OF PEAK TEMPERATURES AROUND REFERENCE VALUES

Parameter	Full-load loss Q_{FL}	Oil level $\%_{h(T),int}$	$k_{Gc} = k_{Gf}$	T_{inf}	
Unit	W	% of $h_{T,int}$	$W \cdot m^{-1} \cdot K^{-1}$	$^{\circ}C$	
For a variation of:	+400 (10.7 %)	+10 (11.1 %)	+1 (66.7 %)	+10	
...around a reference of:	3740	90	1.5	11.1	
...the corresponding relative variation in peak temperature [$^{\circ}C$] is:	CL	+6.7	-2.3	-1	+0.43
	CR	+6	-1.5	-1	+0.43
	O	+5.3	0	-1	+0.43
	T	+4	0	-1	+0.57
	Vi	+1.3	0	-2.5	+1.4
	V	+1.3	0	-3	+1.6
	Gc	+0.67	0	-3	+2.4
Gf	0	0	0	+9.7	

Only the parameters which are relatively sensitive to variations are given. It has been found that all other sensitivities are negligible even for relatively large changes in the parameters. The results are similar when it comes to the sensitivity of the average temperatures instead of peak ones. The higher the sensitivity, the darker the cell. It can be noticed that each parameter influences in a different manner the temperature of the elements:

- For an overestimation of the full-load losses, the temperatures increase (especially T_{CR} , T_{CL} and T_O) since more heat is input into the system.
- For an overestimation of the oil level, T_{CR} and T_{CL} decrease, since the total heat capacity of the oil is increased.
- For an overestimation of the surrounding ground's thermal conductivity, the temperatures are decreased (especially T_{Gc} and T_V) since the resistance to the heat flow is obviously decreased. Note that T_{Gf} is not affected because its thickness (20 ft) has been selected precisely in order to include a volume encompassing the full reach of the model; hence, all heat is always dissipated inside Gf , but a thicker Gf makes a lumped parameter model impractical.
- For an overestimation of the boundary ground temperature, the closer an element is to that boundary, the more its temperature is increased.

From Table III, one can see that the two parameters with the greatest influence in the temperature rise of transformers installed in vaults are the full-load heat loss and the surrounding soil temperature. Therefore, rough estimations of other parameters can be used in the model without greatly influencing the results. Nevertheless, looking at the results of Section VI, even when a certain parameter is not known, it is better to use an estimated value rather than removing it from the model because then large errors can occur.

VII. COMMENTS AND CONCLUSIONS

A thermal model for transformers installed in rectangular vaults has been proposed. The model has been validated against onsite measurements on three different transformers with varied sizes and installation characteristics. The average absolute difference between the simulated and measured temperatures

TABLE IV
VALUES OF THE GEOMETRICAL PARAMETERS

Interface	x	Total area		Convection parameters	
		$A_{x,hu} = A_{x,hd}$	$A_{x,v}$	$P_{x,hu} = P_{x,hd}$	$L_x = H_x$
Core/coils	$CR:CL$	Oil in between	$8\pi R^2$	No convection	
Core/oil	CR	$\frac{128}{9}R^2$	$\frac{320}{3\sqrt{3}}R^2$	$\frac{40}{3}R$	$\frac{8}{\sqrt{3}}R$
Coils/oil	CL	$\frac{1}{3}\pi R^2$	$12\pi R^2$	$10\pi R^2$	$2R$

TABLE V
VALUES OF OTHER PARAMETERS

Parameter	Value	Unit	Comment
σ	$5.6704 \cdot 10^{-8}$	$W \cdot K^{-4} \cdot m^{-2}$	Stefan-Boltzmann constant
g	9.812865328	$m \cdot s^{-2}$	Average gravity acceleration
ε_T	0.85	\emptyset	Stainless steel, weathered
ε_V	0.94	\emptyset	Concrete, rough
Q_{FL}	3740	W	For transformer 1
Q_{NL}	1271		(see Fig. 10)

over the entire span of this study (one year) is typically less than $4^{\circ}C$. The predicted temperatures are remarkably close to the measured average real temperatures considering the uncertainties in the available data.

It has been shown with parametric studies that all features in the model contribute to the accuracy of the results; hence, none can be removed to simplify the model without losing confidence in the results. With the exception of the full-load heat loss and the surrounding soil temperature, the use of typical (or estimated) values does not greatly affect the results.

APPENDIX

A. System Equations

The details of the system of equations, based on the formulas developed above in (1)–(7), are given in Figs. 10 and 11.

B. Parameters

The transformer geometrical model has been made to depend on only one scaling parameter: the radius of the coils R (see Fig. 2), which is calculated using:

$$Vol_O + Vol_{CR}(R) + Vol_{CL}(R) = \%_{H(T),int} \cdot Vol_{T,int} \quad (12)$$

where

- Vol_O volume of oil poured by the manufacturer;
- $\%_{H(t),int}$ estimated level of the oil along the vertical dimension (height) of the tank;
- $Vol_{T,int}$ total volume inside the tank.

Formulas are given in Fig. 2 for V_{CR} and V_{CL} . Finally, the values of the geometrical parameters are given in Tables IV and V.

ACKNOWLEDGMENT

The authors would like to thank M. Libin for the time spent providing precious experimental and load data.

REFERENCES

- [1] A. M. Lockie and D. K. Whirlow, "Thermal performance of distribution transformers in underground vaults: I—The problem," *IEEE Trans. Power App. Syst.*, vol. PAS-87, no. 9, pp. 1741–1745, Sep. 1968.
- [2] P. S. Yeh, "Heat transfer problems of distribution transformers in open underground vaults," *IEEE Trans. Power App. Syst.*, vol. PAS-90, no. 5, pp. 2391–2398, Sep. 1971.
- [3] D. K. Whirlow and A. M. Lockie, "Thermal performance of distribution transformers in underground vaults: II—Mathematical model," *IEEE Trans. Power App. Syst.*, vol. PAS-87, no. 9, pp. 1745–1754, Sep. 1968.
- [4] MathWorks. Natick, MA, Product Documentation—Matlab—ode23, ode45, ode113, ode15s, ode23s, ode23t, ode23tb—Algorithms. [Online]. Available: <http://www.mathworks.com/help/techdoc/ref/ode45.html>
- [5] D. W. Green and R. H. Perry, "Section 5—Heat and mass transfer," in *Perry's Chemical Engineers' Handbook*, 8th ed. New York: McGraw-Hill, 2007, pp. 5.8–5.13.
- [6] Comsol, Comsol 3.5's Material Library. 2010. [Online]. Available: <http://www.comsol.com/products/material-library/>
- [7] J. F. Lindsay, "Temperature rise of an oil-filled transformer with varying load," *IEEE Trans. Power App. Syst.*, vol. PAS-103, no. 9, pp. 2530–2536, Sep. 1984.



Julien Pierre Albert Sandraz was born in Chambéry, Savoie, France. He received the M.Sc. degree in telecommunications engineering from INSA Lyon, Villeurbanne, France, in 2010, the M.Sc. degree in electrical engineering from the Polytechnic Institute of New York University, Brooklyn, NY, USA, and is currently pursuing the Ph.D. degree in electrical engineering with a concentration in power systems at the Polytechnic Institute of New York University, focusing on nonlinear multiphase active and reactive power definitions and measurements.



Francisco de León (S'86–M'92–SM'02) received the B.Sc. and M.Sc. (Hons.) degrees in electrical engineering from the National Polytechnic Institute, Mexico City, Mexico, in 1983 and 1986, respectively, and the Ph.D. degree in electrical engineering from the University of Toronto, Toronto, ON, Canada, in 1992.

He has held several academic positions in Mexico and has worked for the Canadian electric industry. Currently, he is an Associate Professor at the Polytechnic Institute of New York University, Brooklyn, NY, USA. His research interests include the analysis of power definitions under nonsinusoidal conditions, the transient and steady-state analyses of power systems, the thermal rating of cables and transformers, and the calculation of electromagnetic fields applied to machine design and modeling.



Joseph Cultrera received the B.S. degree in electrical engineering from City College of New York, New York, USA, in 1966.

He is with the Consolidated Edison Company of New York, Inc., New York, USA, where he has held several technical and engineering positions and is currently a Technical Specialist and Senior Engineer in the Distribution Department. He has been involved in several projects regarding the security and reliability of low-voltage underground distribution networks.